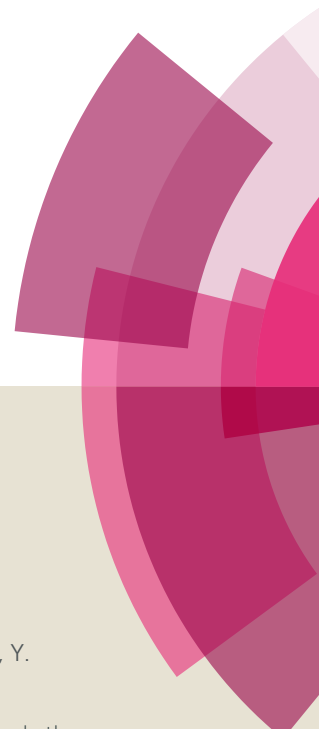


NJC

Accepted Manuscript



This article can be cited before page numbers have been issued, to do this please use: J. Sun, Z. Chen, Y. Xue and J. Chen, *New J. Chem.*, 2018, DOI: 10.1039/C7NJ03904B.



This is an Accepted Manuscript, which has been through the Royal Society of Chemistry peer review process and has been accepted for publication.

Accepted Manuscripts are published online shortly after acceptance, before technical editing, formatting and proof reading. Using this free service, authors can make their results available to the community, in citable form, before we publish the edited article. We will replace this Accepted Manuscript with the edited and formatted Advance Article as soon as it is available.

You can find more information about Accepted Manuscripts in the [author guidelines](#).

Please note that technical editing may introduce minor changes to the text and/or graphics, which may alter content. The journal's standard [Terms & Conditions](#) and the ethical guidelines, outlined in our [author and reviewer resource centre](#), still apply. In no event shall the Royal Society of Chemistry be held responsible for any errors or omissions in this Accepted Manuscript or any consequences arising from the use of any information it contains.



Journal Name

ARTICLE

Design and construction of Ni_{3-x}Co_xO₄ nanorods grown on Ni foam for tuning synthetic natural gas heating value

Jiaqiang Sun, * Zheng Chen, Yingying Xue, and Jiangang Chen*

Received 00th January 20xx,
Accepted 00th January 20xx

DOI: 10.1039/x0xx00000x

www.rsc.org/

The Ni_{3-x}Co_xO₄ nanorods with different Ni/Co ratio have been fabricated on Ni foam by a controllable process. The conversion of CO for Ni₂CoO₄ nanorods was the highest during the whole methanation reaction processing. The design of the Ni_{3-x}Co_xO₄ nanorods with different Ni/Co ratio is the origin of the different catalytic activity. The synergetic effect of Ni and Co also tunes the product selectivity, and thus controlling the heating value of synthetic natural gas. The nanorods directly grown on the Ni foam can ensure efficient anchoring of the nanorods. The designed synthesis of the Ni_{3-x}Co_xO₄ nanorods with different Ni/Co ratio provides new strategy for controlling the catalytic activity and selectivity of syngas methanation.

1. Introduction

Methanation is a chemical process used to generate methane from a mixture of hydrogen and carbon monoxide (syngas), which can be derived from non-petroleum feedstocks such as coal, biomass and even coke oven gas.^{1, 2} Previously, methanation reactions were used for the removal of carbon monoxide from feed gas in ammonia synthesis. Production of synthetic natural gas (SNG) by syngas methanation has been considered as a promising way towards the sustainable development and clean utilization of coal.³ Recently, methanation has received attention in the production of high calorie SNG.^{4, 5} The traditional catalyst for methanation is supported nickel catalysts. Various supported nickel catalysts have been explored extensively for the methanation process.⁶⁻⁸ Nickel still has a high activity and a comparatively low price, but nickel catalysts yield nearly pure methane gas as the product and so the heating value of the product gas is considerably low.⁹ In order to extend the application of natural gas as town gas, it is extremely important to improve the heating value. To achieve a high heating value, a proper amount of C₂₋₄ paraffins, which have greater heating values than methane, must be formed during the methanation process. Therefore, selectivity control is one of the key challenges of research into methanation. So the methanation catalyst should be modified by the Fischer–Tropsch (FT) catalysts in a controlled manner. Cobalt catalysts are generally more selective to linear longchain hydrocarbons, which have been employed in industry for FT synthesis.¹⁰ Researchers found that Co–Mn–Ru/Al₂O₃ showed the best performance in

the conversion of coke oven gas (21.2 MJ/Nm³) into high-calorie SNG (41.9 MJ/Nm³) on a fluidized bed reactor.¹¹ It is noted that syngas methanation is a strongly exothermic process and undesired hotspots often arise in the reactor bed, which makes the temperature-control difficult and even shortens the catalyst lifetime.¹² Although various technologies are proposed for solving the limitation of heat transfer, some other challenges arise simultaneously. Thus, designing and synthesizing novel catalysts with high reactivity and stability for developing an energy-efficient SNG process is particularly desirable. Metal foam catalysts with inherent outstanding features such as interconnected porous structure, favourable mass/heat transfer, low pressure drop and desired mechanical robustness, have been attracting growing interests in heterogeneous catalysis.^{13, 14} The metal foams are opening an opportunity on the development of novel catalyst and reactor technology for the SNG process from syngas, but effective and efficient non-coating method for placing catalytic active sites onto the surface of metal foam is particularly desirable and is still a significantly challenge.^{15, 16} The development of nanotechnology in recent decades brings new opportunities in the exploration of high-performance catalysts.^{17, 18} Herein, we report controllable synthesis of the Ni_{3-x}Co_xO₄ nanorods grown on Ni foam via a hydrothermal process of precursor and subsequent thermal decomposition. The Ni_{3-x}Co_xO₄ nanorods with different Ni/Co ratios were studied in the syngas methanation reaction. The activities of the catalysts were evaluated in terms of CO conversion, C₂₋₄ selectivity and heating value based on the produced hydrocarbons. The designed synthesis of the Ni_{3-x}Co_xO₄ nanorods with different Ni/Co ratios provides new strategy with an aim at controlling the catalytic activity and selectivity for syngas methanation.

State Key Laboratory of Coal Conversion, Institute of Coal Chemistry, Chinese Academy of Sciences, Taiyuan, 030001, China
E-mail: chenjq@sxicc.ac.cn; sunjiaqiang@sxicc.ac.cn.

2. Experimental

2.1 Catalyst Preparation

A mixture of $\text{Co}(\text{NO}_3)_2 \cdot 6\text{H}_2\text{O}$, $\text{Ni}(\text{NO}_3)_2 \cdot 6\text{H}_2\text{O}$ (metal ions total concentration, 0.1 M; $[\text{Ni}^{2+}]/[\text{Co}^{2+}] = 0, 0.5, 1.0, 2.0$ or 0.1M Ni^{2+}) and 50 mmol of $\text{CO}(\text{NH}_2)_2$ were dissolved in 100 mL of water under magnetic stirring. The homogeneous solution prepared above was transferred directly into a 200 mL Teflon-lined stainless steel autoclave. The Ni foam (1 g) was carefully cleaned with HCl (1 mol/L), absolute ethanol, and distilled water, and immersed in the homogeneous solution. The autoclave was sealed and maintained at 120 °C for 8 h and then allowed to cool down to room temperature naturally. The catalysts grown on Ni foam was washed several times with distilled water, dried at 80 °C for 4 h, and calcinated at 400 °C for 4 h in air, but the NiO precursor was calcinated in N_2 . Finally the produced catalysts were reduced at 500 °C and 0.2 MPa for 4 h by H_2 with a gas hourly space velocity (GHSV) of 10 L/h/g in a fixed-bed reactor.

2.2 Characterization

In order to characterize the catalysts, the samples were prepared by scraping the $\text{Ni}_{3-x}\text{Co}_x\text{O}_4$ from the Ni foam. Powder X-ray diffraction (XRD) was performed on a Shimadzu XRD-6000 diffractometer with Cu $\text{K}\alpha$ radiation ($\lambda = 1.5418 \text{ \AA}$) in the 2θ range from 10° to 70°. The morphology and size of as-synthesized samples were monitored by using a scanning electron microscope (SEM, Zeiss Supra 55). The structure and composition of the products were characterized by means of a high-resolution transmission electron microscope (HRTEM, JEM 2100F) and energy dispersive X-ray spectroscopy (EDS). The surface area was determined by BET (Brunauer–Emmett–Teller) measurements using a Tristar II 3020 N_2 adsorption analyser. The precursor (50 mg) was placed in a quartz reactor and was reduced by a 5% H_2/N_2 gas mixture at a flow rate of 50 mL/min, as the TPR experiments were performed. The temperature was ramped at 10 °C/min to the final

temperature and the hydrogen consumption was recorded using a thermal conductivity detector (TCD).

2.3 Catalytic Reaction

The catalytic behaviour was investigated in a fixed bed reactor. The reactor can be supplied with H_2 , synthesis gas ($n_{\text{H}_2}/n_{\text{CO}}=2$). The gas flow is controlled by Brooks 5850E mass flow controllers (MFC). The pressure is controlled via a back pressure regulator. The reaction products pass a 130 °C hot trap and a 5 °C cooling trap at working pressure and can be measured online by a GC. After in-situ reduction, the reactor was cooled to 50 °C, the synthesis gas ($n_{\text{H}_2}/n_{\text{CO}}=2$, GHSV = 5 L/h/g) was fed into the catalysts bed and the temperature was increased at 1.0 °C/min heating rate to 300 °C. During testing, the pressure of synthesis gas was maintained at 2.0 MPa. The reaction rates and hydrocarbon selectivity were evaluated after 24 h on-stream. The gaseous reaction products were analysed on-line by gas chromatography (GC 920).

3. Results and discussion

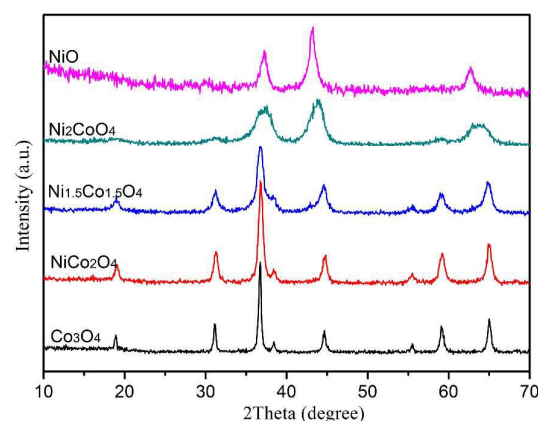


Figure 1 XRD patterns of the $\text{Ni}_{3-x}\text{Co}_x\text{O}_4$ nanorods with different Ni/Co ratio.

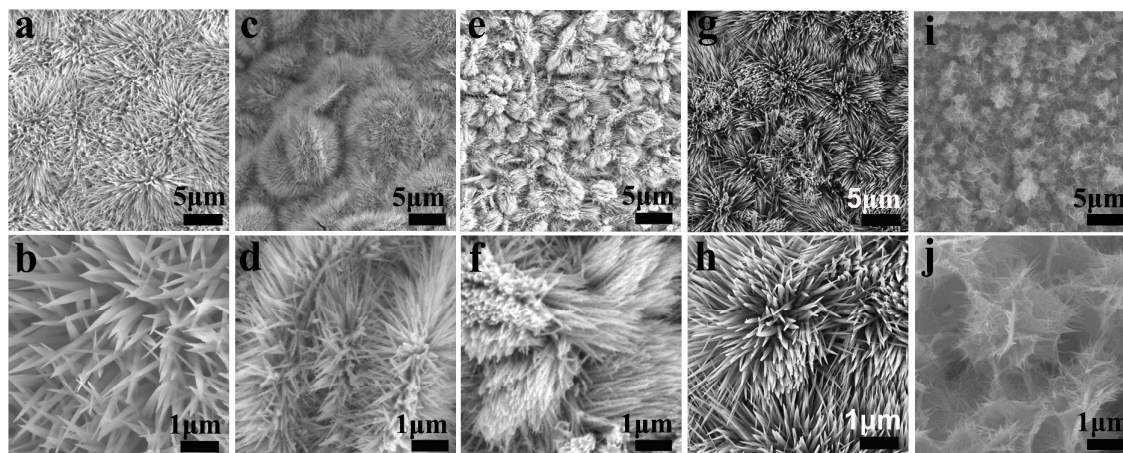


Figure 2 SEM images of the catalysts formed on the Ni foam with different Ni/Co ratio: Co_3O_4 (a, b), NiCo_2O_4 (c, d), $\text{Ni}_{1.5}\text{Co}_{1.5}\text{O}_4$ (e, f), Ni_2CoO_4 (g, h) and NiO (i, j).

Journal Name

ARTICLE

The $\text{Ni}_{3-x}\text{Co}_x\text{O}_4$ nanorod arrays on Ni foam were achieved by a stepwise transformation process based on fabrication of hierarchical $\text{Co}_{3-x}\text{Fe}_x\text{O}_4$ nanowire arrays on an iron substrate.^{19, 20} A piece of nickel foam was immersed in a solution containing a mixture of Co^{2+} and Ni^{2+} ions and urea. First, by using urea as the mineralizer and undergoing an easily controllable hydrothermal process, a thin film of precursor has been successfully attained on Ni foam. Second, after the adequate pyrolysis of precursors at 400 °C in air or N_2 for 4 h, $\text{Ni}_{3-x}\text{Co}_x\text{O}_4$ nanorod arrays can be obtained with a robust mechanical adhesion to the Ni foam. Figure 1 show the XRD patterns of the as-prepared samples. All the diffraction peaks of Co_3O_4 can be indexed to cubic phase, which is consistent with the value in the standard card (JCPDS Card No. 43-1003). All the diffraction peaks of NiCo_2O_4 can be indexed to cubic phase, which is consistent with the value in the standard card (JCPDS Card No. 20-0781). With the increasing of Ni/Co ratios, all the peaks of $\text{Ni}_{1.5}\text{Co}_{1.5}\text{O}_4$ and Ni_2CoO_4 have slightly smaller 2θ values compared with the XRD pattern of NiCo_2O_4 , which can be attributed to the substitution of some of the cobalt ions by nickel in $\text{Ni}_{3-x}\text{Co}_x\text{O}_4$. Furthermore, all the diffraction peaks of NiO also can be indexed to cubic phase, which is consistent with the value in the standard card (JCPDS Card No. 47-1049). The SEM images in Figure 2 clearly show the morphology of the $\text{Ni}_{3-x}\text{Co}_x\text{O}_4$ nanorods directly grown on the Ni foam. The gathered $\text{Ni}_{3-x}\text{Co}_x\text{O}_4$ nanorod arrays with a relatively high density are obviously observed, especially, the NiO possess rod-on-sheet architecture. According to the high-magnification images, the average diameter and length of the $\text{Ni}_{3-x}\text{Co}_x\text{O}_4$ nanorods with a sharp tip are estimated to be about 100 nm

and 2 μm , respectively. Figure 3 displays TEM images of near the tip of the $\text{Ni}_{3-x}\text{Co}_x\text{O}_4$ nanorods, from which we can find that, a large number of cracks and pores exist on the surface of the nanorods. HRTEM were used to further confirm the phase of the nanorods. Figure 3b shows a HRTEM image taken from the Co_3O_4 nanorod, which indicates a lattice spacing of 0.286 nm, corresponding to the (220) crystal planes of Co_3O_4 , in good agreement with the original XRD pattern in Figure 1. The interplanar spacing of 0.287 nm was detected for an individual NiCo_2O_4 nanorod, corresponding to the (220) crystal planes of NiCo_2O_4 (Figure 3d). As shown in Figures 3f, an interplanar spacing of 0.203 nm was detected for an individual nanorod, corresponding to the (400) crystal planes of $\text{Ni}_{1.5}\text{Co}_{1.5}\text{O}_4$. The interplanar spacing of 0.288 nm was detected for an individual Ni_2CoO_4 nanorod, corresponding to the (220) crystal planes of Ni_2CoO_4 (Figure 3h). The interplanar spacing of 0.241 nm was detected for an individual NiO nanorod, corresponding to the (111) crystal planes of NiO (Figure 3j). The EDS was conducted in-situ with the HRTEM to analyze the composition of the $\text{Ni}_{3-x}\text{Co}_x\text{O}_4$ nanorods (Figure 4). The $\text{Ni}_{3-x}\text{Co}_x\text{O}_4$ nanorods contained Co, Ni and O atoms, which shows the atomic ratio of Ni/Co of NiCo_2O_4 , $\text{Ni}_{1.5}\text{Co}_{1.5}\text{O}_4$ and Ni_2CoO_4 nanorods to be around 0.66, 1.00 and 2.10, respectively.

The reduction behavior of the $\text{Ni}_{3-x}\text{Co}_x\text{O}_4$ nanorods was investigated by H_2 -TPR and the profiles are shown in Figure 5. There are two peaks in the temperature range between 150 °C and 450 °C for Co_3O_4 . The smaller peak centered at 230 °C can be attributed to the reduction process of Co^{3+} to Co^{2+} . The larger peak centered at 335 °C can be attributed to the reduction of Co^{2+} to Co^0 .

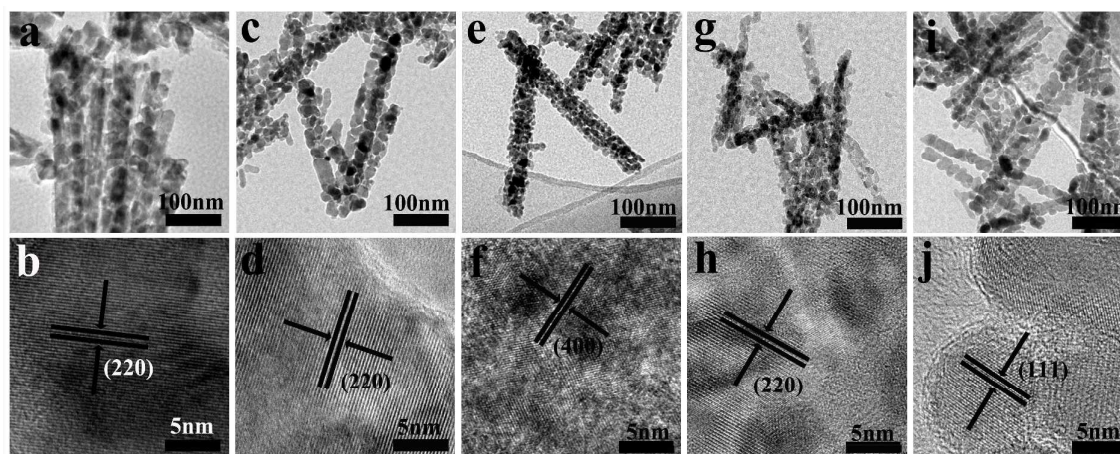


Figure 3 TEM (a) and HRTEM (b) images of the Co_3O_4 nanorods; TEM (c) and HRTEM (d) images of the NiCo_2O_4 nanorods; TEM (e) and HRTEM (f) images of the $\text{Ni}_{1.5}\text{Co}_{1.5}\text{O}_4$ nanorods; TEM (g) and HRTEM (h) images of the Ni_2CoO_4 nanorods; TEM (i) and HRTEM (j) images of the NiO nanorods.

Journal Name

ARTICLE

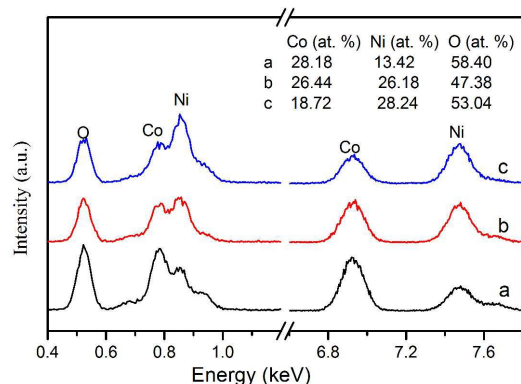


Figure 4 EDS spectra of NiCo₂O₄ (a), Ni_{1.5}Co_{1.5}O₄ (b) and Ni₂CoO₄ (c) nanorods.

There are four peaks in the temperature range between 150 °C and 450 °C for NiCo₂O₄, Ni_{1.5}Co_{1.5}O₄ and Ni₂CoO₄. They are distinguished corresponding to the consecutive stepwise reduction of Co³⁺, Ni³⁺, Co²⁺ and Ni²⁺. For the NiCo₂O₄ nanorods, the peak centered at 265 °C can be attributed to the reduction process of Co³⁺ to Co²⁺; the peak centered at 303 °C can be attributed to the reduction process of Ni³⁺ to Ni²⁺; The peak centered at 373 °C can be attributed to the reduction of Co²⁺ to Co⁰; The peak centered at 423 °C can be attributed to the reduction of Ni²⁺ to Ni⁰. With the increase of Ni and Co ratios, the reduction peak shifted slightly to lower temperature. For the Ni_{1.5}Co_{1.5}O₄ nanorods, there are two peaks centered at 245 °C and 270 °C can be attributed to the reduction process of Co³⁺ and Ni³⁺; while the larger peak centers at 341 °C and 392 °C can be attributed to the reduction process of Co²⁺ and Ni²⁺, respectively. For the Ni₂CoO₄ nanorods, there are two smaller peaks centered at 228 °C and 248 °C, and two larger peak centered at 319 °C and 381 °C, corresponding to the reduction

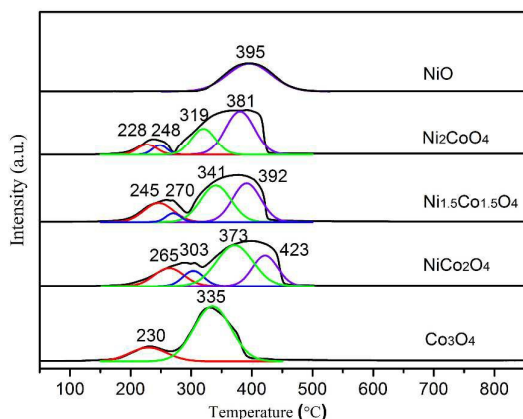


Figure 5 H₂-TPR profiles of the Ni_{3-x}Co_xO₄ nanorods with different Ni/Co ratio.

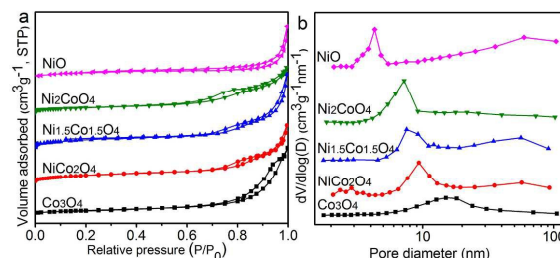


Figure 6 Nitrogen adsorption-desorption isotherms (a) and pore size distributions (b) of the Ni_{3-x}Co_xO₄ nanorods with different Ni/Co ratio.

of Co³⁺, Ni³⁺, Co²⁺ and Ni²⁺, respectively. For the NiO nanorods, there is only one peak centered at 395 °C, which can be attributed to the reduction process of Ni²⁺ to Ni⁰. N₂ adsorption-desorption isotherms measurements were used to determine the specific surface area, average pore size and pore volume of the Ni_{3-x}Co_xO₄ nanorods. Figure 6 shows the N₂ adsorption-desorption isotherms and the corresponding pore size distributions of the Ni_{3-x}Co_xO₄ nanorods. The BET surface areas of Co₃O₄, NiCo₂O₄, Ni_{1.5}Co_{1.5}O₄, Ni₂CoO₄ and NiO nanorods were calculated to be 62.2 m²/g, 64.7 m²/g, 79.9 m²/g, 62.6 m²/g and 62.5 m²/g, respectively. The total pore volumes of Co₃O₄, NiCo₂O₄, Ni_{1.5}Co_{1.5}O₄, Ni₂CoO₄ and NiO nanorods were calculated to be 0.31 cm³/g, 0.26 cm³/g, 0.32 cm³/g, 0.21 cm³/g and 0.20 cm³/g, respectively. The pore size distribution curves of the Ni_{3-x}Co_xO₄ nanorods derived from the desorption curves of the Barrett-Joyner-Halenda model. It can be clearly seen that the pores centered at around 17 nm, 9 nm, 8 nm, 7 nm and 4 nm were attributed to the mesoporous of Co₃O₄, NiCo₂O₄, Ni_{1.5}Co_{1.5}O₄, Ni₂CoO₄ and NiO nanorods, respectively (Fig. 6b).

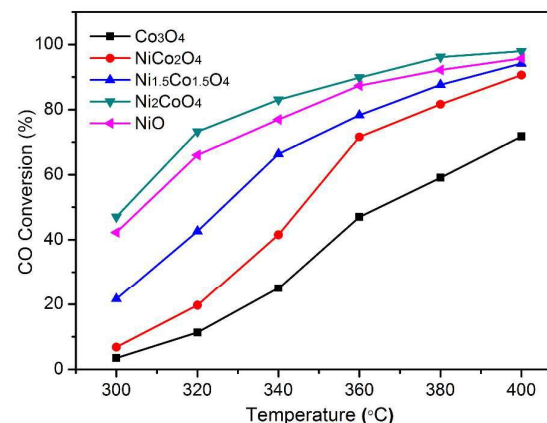


Figure 7 CO conversion profiles of NiCo₂O₄ (a), Ni_{1.5}Co_{1.5}O₄ (b) and Ni₂CoO₄ (c) nanorods. Reaction conditions: catalyst 1.0 g P=2.0 MPa, H₂/CO=2, GHSV=5 L·g⁻¹·h⁻¹

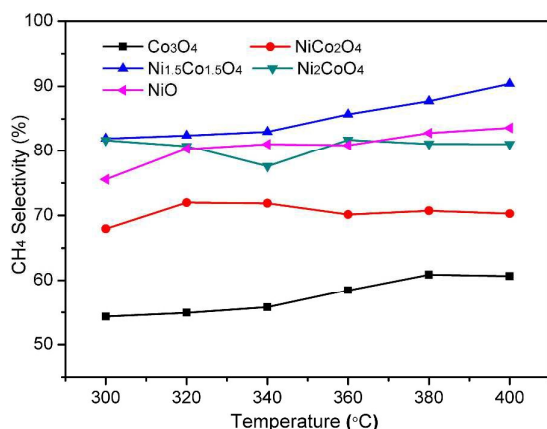


Figure 8 CH₄ selectivity profiles of the Ni_{3-x}Co_xO₄ nanorods catalysts with different Ni/Co ratio. Reaction condition: catalyst 1.0 g P=2.0 MPa, H₂/CO=2, GHSV=5 L·g⁻¹·h⁻¹

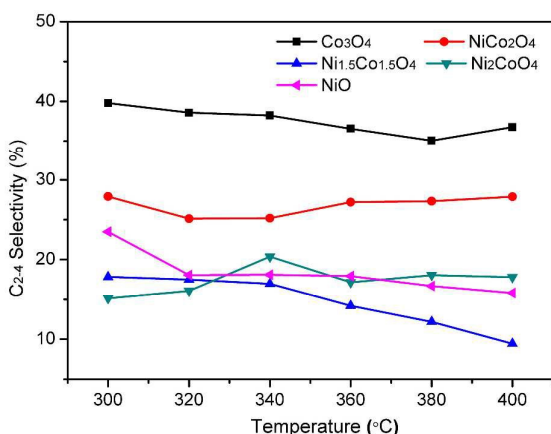


Figure 9 C₂₋₄ selectivity profiles of the Ni_{3-x}Co_xO₄ nanorods catalysts with different Ni/Co ratio. Reaction condition: catalyst 1.0 g P=2.0 MPa, H₂/CO=2, GHSV=5 L·g⁻¹·h⁻¹

Figure 7 shows the catalytic performance of the Ni_{3-x}Co_xO₄ nanorods with different Ni/Co ratio for the syngas methanation. It can be seen from Figure 7 that the conversion of CO over the catalyst increases with increasing reaction temperature. A significant difference in CO conversion was observed in the Ni_{3-x}Co_xO₄ nanorods. Among the tested catalysts, Co₃O₄ nanorods exhibit the lowest activity and the CO conversion is 3.5% at 300 °C. However, the CO conversion is 6.8% over NiCo₂O₄ nanorods, 21.6% over Ni_{1.5}Co_{1.5}O₄

nanorods, 47.0% over Ni₂CoO₄ nanorods and 42.3% over NiO nanorods at 300 °C, respectively.

At the same reaction conditions, with the increasing of mole ratio of Ni and Co, the CO conversion increased obviously, indicating that Ni specie is more active than Co species for CO methanation reaction.²¹ The Ni content is a significant influence factor among other factors for catalyst.²² At 400 °C, Co₃O₄, NiCo₂O₄, Ni_{1.5}Co_{1.5}O₄, Ni₂CoO₄ and NiO nanorods showed the highest conversion of CO, which was 71.7%, 90.6%, 94.2%, 97.9%, and 95.7%, respectively. The conversion of CO for Ni₂CoO₄ nanorods was the highest during the whole reaction processing, which might be mainly attributed to the synergetic effect between Ni and Co. The design of the Ni_{3-x}Co_xO₄ nanorods with different Ni/Co ratio is the origin of the different catalytic activity. The selectivity (expressed as mol% without CO₂) of the Ni_{3-x}Co_xO₄ nanorods with temperature on stream are shown in Figure 8 and Figure 9. The Ni_{3-x}Co_xO₄ nanorods catalysts mainly produce light alkane. CH₄ and C₂₋₄ are the main component in the hydrocarbon products. It can be seen that the CH₄ selectivity of Co₃O₄ nanorods is 54.3% at 300 °C; The CH₄ selectivity of NiCo₂O₄ nanorods is 67.9% at 300 °C, when further increasing Ni proportion, the CH₄ selectivity of the Ni_{1.5}Co_{1.5}O₄ nanorod catalysts increases to 81.9% at 300 °C. The CH₄ selectivity of Ni₂CoO₄ nanorods is similar with that of Ni_{1.5}Co_{1.5}O₄ nanorods at 300 °C. While the CH₄ selectivity of NiO nanorods is 75.6% at 300 °C, which is lower than that of Ni_{1.5}Co_{1.5}O₄ and Ni₂CoO₄ nanorods. The selectivity of CH₄ over all the catalysts except for Ni₂CoO₄ increases slightly with increasing reaction temperature. With the increasing of temperature, the selectivity of CH₄ is up to 90% over Ni_{1.5}Co_{1.5}O₄ nanorods. The Co₃O₄ nanorods show the lowest CH₄ selectivity compared with the bimetallic catalysts and NiO at all the temperature ranges. Figure 9 shows C₂₋₄ selectivity profiles of the Ni_{3-x}Co_xO₄ nanorods catalysts with different Ni/Co ratio. The Co₃O₄ nanorods show the highest C₂₋₄ selectivity at 300 °C. When further decreasing Co proportion, the C₂₋₄ selectivity of the bimetallic catalysts decreases and the Ni₂CoO₄ catalyst shows the lowest selectivity at 300 °C. It can be seen that C₂₋₄ selectivity of Ni₂CoO₄ is similar with that of NiO above 320 °C. Furthermore, the selectivity of C₅₊ over all of the Ni_{3-x}Co_xO₄ nanorods is very low.

The SNG calorific value produced from Co₃O₄, NiCo₂O₄, Ni_{1.5}Co_{1.5}O₄, Ni₂CoO₄ and NiO nanorods was calculated (Table 1), with the heating value of 62.4 MJ/Nm³, 56.6 MJ/Nm³, 44.0 MJ/Nm³, 50.0 MJ/Nm³ and 48.3 MJ/Nm³, respectively. The highest heating value of Co₃O₄ nanorods was ascribed to the highest C₂₊ hydrocarbons content.

Table 1. Product distributions of catalysts in methanation reaction.

Journal Name

ARTICLE

Catalysts	Q (MJ/Nm ³)	CO conv. (%)	Selectivity (%)				
			CH ₄	C ₂ H ₆	C ₃ H ₈	C ₄ H ₁₀	C ₅₊
Co ₃ O ₄	62.4	71.7	60.6	17.4	11.5	7.8	2.7
NiCo ₂ O ₄	56.6	90.6	69.4	15.5	8.5	4.6	2.0
Ni _{1.5} Co _{1.5} O ₄	44.0	94.2	90.3	6.8	1.8	0.9	0.2
Ni ₂ CoO ₄	50.0	97.9	80.0	11.3	5.5	1.8	1.4
NiO	48.3	95.7	83.6	9.2	4.0	2.6	0.6

Reaction conditions: catalyst 1.0 g T= 400 °C, P=2.0 MPa, H₂/CO=2, GHSV=5 L·g⁻¹·h⁻¹

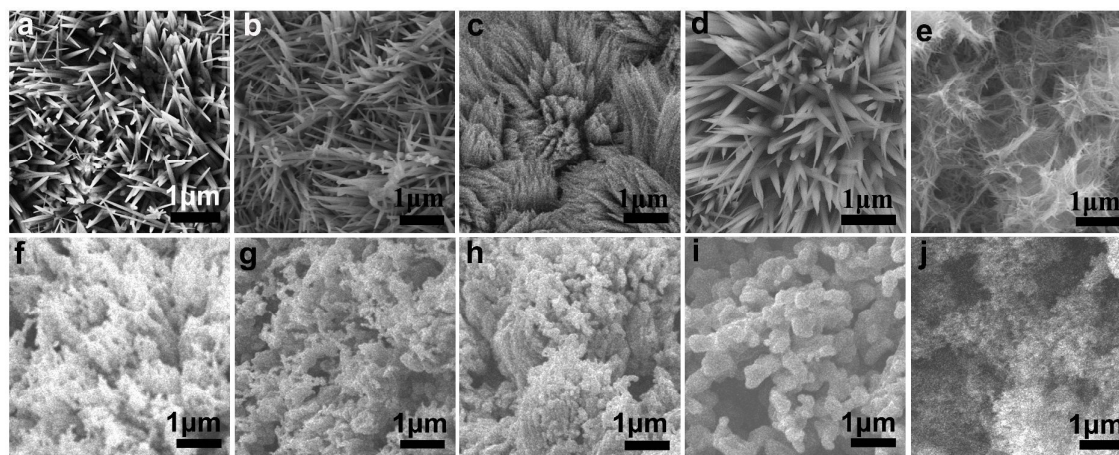


Figure 10 SEM images of Co₃O₄ (a), NiCo₂O₄ (b), Ni_{1.5}Co_{1.5}O₄ (c), Ni₂CoO₄ (d) and NiO (e) nanorod catalysts after reduction; SEM images of Co₃O₄ (f), NiCo₂O₄ (g), Ni_{1.5}Co_{1.5}O₄ (h), Ni₂CoO₄ (i) and NiO (j) nanorod catalysts after reaction.

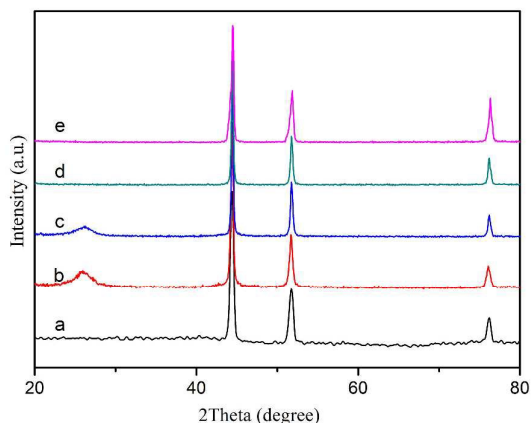


Figure 11 XRD pattern of Co₃O₄ (a), NiCo₂O₄ (b), Ni_{1.5}Co_{1.5}O₄ (c), Ni₂CoO₄ (d) and NiO (e) nanorod catalysts used.

Figure 10 shows SEM images of Co₃O₄, NiCo₂O₄, Ni_{1.5}Co_{1.5}O₄, Ni₂CoO₄ and NiO nanorods after reduction and reaction. From the images, it can be seen that there is no larger changing in

the morphology after reduction, but the nanorods change into small particles after reaction, due to sintering in the reaction process. The phase characterization of the catalysts used on stream was examined by XRD (Figure 11). The cubic phase Co appear in the XRD patterns for the Co₃O₄ nanorods catalysts used, which is consistent with the value in the standard card (JCPDS 01-1260). The cubic phase Ni appear in the XRD patterns for the NiO nanorods catalysts used, which is consistent with the value in the standard card (JCPDS 15-0806). The cubic phase CoNi appear in the XRD patterns for the NiCo₂O₄, Ni_{1.5}Co_{1.5}O₄ and Ni₂CoO₄ nanorods catalysts used, which is very similar to those of either fcc Ni (JCPDS 15-0806) or fcc Co (JCPDS 01-1260) while a slight variation for the peak position can be observed and all the peak positions lie between that of pure fcc Ni and pure fcc Co. (Figure 9).^{23, 24} Furthermore, the carbon peak appear in the XRD patterns for NiCo₂O₄ and Ni_{1.5}Co_{1.5}O₄, which is due to the coke in the surface of the catalysts, while there is no carbon peaks for other catalysts. Experimental results have indicated that, the syngas methanation proceed on metallic Ni species, which is especially active in methanation.⁸

In addition, there is currently a consensus in the literature that Fischer–Tropsch synthesis proceeds on cobalt metal particles.^{10, 20} Therefore, the interaction between Ni and Co might improve the adsorption and activation of CO and thus enhance the methanation activity of the $\text{Ni}_{3-x}\text{Co}_x\text{O}_4$ catalysts. The formation of C_{2+} hydrocarbons is suppressed for nickel-based catalysts, therefore the heating value of the product gas is considerably low for nickel-based catalysts.⁹ But Co-based catalysts are generally more selective to linear longchain hydrocarbons.^{25, 26} In consequence, the synergetic effect of Ni and Co tunes the product selectivity, and thus controlling the heating value of the product. The nanorods directly grown on the Ni foam can ensure efficient anchoring of the nanorods and prevent leaching during catalytic reactions. Furthermore, the spaces between neighboring nanorods are much larger, which allows for easy gas diffusion and mass transport, resulting in a high utilization of materials.

Conclusions

In summary, the $\text{Ni}_{3-x}\text{Co}_x\text{O}_4$ nanorods with different Ni/Co ratio have been fabricated on Ni foam by a controllable process involving the hydrothermal growth and calcinations of precursor. The $\text{Ni}_{3-x}\text{Co}_x\text{O}_4$ nanorods show different catalytic activity and selectivity in the syngas methanation reaction. It can be found that the selectivity to methane increase at higher CO conversion levels for $\text{Ni}_{1.5}\text{Co}_{1.5}\text{O}_4$ nanorods. The Ni_2CoO_4 nanorods showed the highest CO conversion and the suitable heating value of product at 400 °C, which were 97.9% and 50.0 MJ/Nm³. The synergetic effect of Ni and Co tuned the product selectivity, and thus controlling the heating value of the product. The present results suggest that specifically designed $\text{Ni}_{3-x}\text{Co}_x\text{O}_4$ nanorods with different Ni/Co ratios by controlling synthesis parameters on Ni foam might bring new opportunities for developing highly efficient catalysts.

Acknowledgements

This work was supported by the National Natural Science Foundation of China (21503256, 21373254), the autonomous research project of State Key Laboratory of Coal Conversion (SKLCC 2013BWZ004).

Notes and references

- J. Kopyscinski, T. J. Schildhauer and S. M. A. Biollaz, *Fuel*, 2010, **89**, 1763-1783.
- M. Gassner and F. Maréchal, *Energy Environ. Sci.*, 2012, **5**, 5768-5789.
- V. M. Lebarbier, R. A. Dagle, L. Kovarik, K. O. Albrecht, X. Li, L. Li, C. E. Taylor, X. Bao and Y. Wang, *Appl. Catal. B: Environ.*, 2014, **144**, 223-232.
- M. Chen, J. Zhou, J. Zhang, J. Zhang, Z. Chen, J. Ding, F. Kong, G. Qian and J. Chen, *Appl. Catal. A: Gen.*, 2017, **534**, 94-100.
- H. L. Yong, D. W. Lee, H. Kim, H. S. Choi and K. Y. Lee, *Fuel*, 2015, **159**, 259-268.
- J. Gao, Q. Liu, F. Gu, B. Liu, Z. Zhong and F. Su, *Rsc Adv.*, 2015, **5**, 22759-22776.
- T. A. Le, M. S. Kim, S. H. Lee, T. W. Kim and E. D. Park, *Catal. Today*, 2017, **293**, 89-96.
- H. Lu, X. Yang, G. Gao, J. Wang, C. Han, X. Liang, C. Li, Y. Li, W. Zhang and X. Chen, *Fuel*, 2016, **183**, 335-344.
- C. Cheng, D. Shen, R. Xiao and C. Wu, *Fuel*, 2017, **189**, 419-427.
- A. Y. Khodakov, W. Chu and P. Fongarland, *Chem. Rev.*, 2007, **107**, 1692-1744.
- T. Inui, A. Sakamoto, T. Takeguchi and Y. Ishigaki, *Ind. Eng. Chem. Res.*, 1989, **28**, 427-431.
- S. Rönsch, J. Schneider, S. Matthischke, M. Schlüter, M. Götz, J. Lefebvre, P. Prabhakaran and S. Bajohr, *Fuel*, 2016, **166**, 276-296.
- J. A. Moulijn, M. T. Kreutzer, T. A. Nijhuis and F. Kapteijn, *Adv. Catal.*, 2011, **54**, 249-327.
- R. J. Farrauto, Y. Liu, W. Ruettinger, O. Ilinich, L. Shore and T. Giroux, *Catal. Rev.*, 2007, **49**, 141-196.
- Y. Li, Q. Zhang, R. Chai, G. Zhao, Y. Liu and Y. Lu, *Chemcatchem*, 2015, **7**, 1427-1431.
- Y. Li, Q. Zhang, R. Chai, G. Zhao, F. Cao, L. Ye and L. Yong, *Appl. Catal. A: Gen.*, 2016, **510**, 216-226.
- S. Liu, L. Hu, X. Xu, A. A. Al - Ghamdi and X. Fang, *Small*, 2015, **11**, 4267.
- Q. Wang, X. Wang, B. Liu, G. Yu, X. Hou, D. Chen and G. Shen, *J. Mater. Chem. A*, 2013, **1**, 2468-2473.
- J. Sun, Y. Li, X. Liu, Q. Yang, J. Liu, X. Sun, D. G. Evans and X. Duan, *Chem. Commun.*, 2012, **48**, 3379-3381.
- J. Sun, S. Zheng, K. Zhang, D. Song, Y. Liu, X. Sun and J. Chen, *J. Mater. Chem. A*, 2014, **2**, 13116-13122.
- M. A. Vannice, *J. Catal.*, 1975, **37**, 449-461.
- S. Hwang, J. Lee, U. G. Hong, J. G. Seo, C. J. Ji, J. K. Dong, H. Lim, C. Byun and I. K. Song, *J. Ind. Eng. Chem.*, 2011, **17**, 154-157.
- M. Cheng, M. Wen, S. Zhou, Q. Wu and B. Sun, *Inorg. Chem.*, 2012, **51**, 1495-1500.
- X. W. Wei, X. M. Zhou, K. L. Wu and Y. Chen, *Crystengcomm*, 2011, **13**, 1328-1332.
- Q. Zhang, J. Kang and Y. Wang, *Chemcatchem*, 2010, **2**, 1030-1058.
- Q. Zhang, K. Cheng, J. Kang, W. Deng and Y. Wang, *Chemsuschem*, 2014, **7**, 1251-1264.

The table of contents entry

Design and construction of $\text{Ni}_{3-x}\text{Co}_x\text{O}_4$ nanorods grown on Ni foam for tuning synthetic natural gas heating value

Jiaqiang Sun, * Zheng Chen, Yingying Xue, and Jiangan Chen*

Keyword ($\text{Ni}_{3-x}\text{Co}_x\text{O}_4$, nanorods, tuning, heating value)

TOC figure

The $\text{Ni}_{3-x}\text{Co}_x\text{O}_4$ nanorods with different Ni/Co ratio have been fabricated on Ni foam, which show excellent catalytic activity and can tune synthetic natural gas heating value.

